Endoplasmic Reticulum Targeting Reactive Oxygen Species Sensor Based on Dihydrofluorescein: Application of Endoplasmic Reticulum Stress

Hoa Thi Le,[†,†] Hye-Ryeong Jo,[‡,†] Se-Yun Oh,[‡] Jinwook Jung,[‡] Young Gi Kim,[‡] Chulhun Kang,[‡,*] and Tae Woo Kim[‡,*]

[†]*Department of Applied Chemistry, College of Applied Sciences, Kyung Hee University, Gyeonggi-do, 449-701, Republic of Korea*
[‡]*Graduate School of East-West Medical Science, Kyung Hee University, Gyeonggi-do, 449-701, Republic of Korea. *E-mail: kangch@khu.ac.kr; tw1275@khu.ac.kr*
Received October 30, 2020, Accepted December 7, 2020, Published online December 18, 2020

Endoplasmic reticulum (ER) has a unique redox environment, which plays critical roles in the organelle's function and in its pathological responses such as ER stress. In this work, we introduce an ER-targeting fluorogenic reactive oxygen species (ROS) chemosensor (ER-Flu) from copper(I)-catalyzed alkyne-azide cycloaddition of 3-propargyl ester of 2′,7′-dichlorodihydrofluorescein diacetate and N_3-glibenclamide, which were adopted as a fluorogenic ROS sensing module and an ER-targeting module, respectively. Thereby, a series of confocal microscopic experiments of ER-Flu demonstrated that the sensor localizes in ER of the live cells and that ROS are elevated in the cells by ER stress inducers such as thapsigargin, brefeldin A, and tunicamycin.

Keywords: Dihydrofluorescein, Endoplasmic reticulum-targeting, Fluorescent chemosensors, Glibenclamide, Reactive oxygen species, ER stress

Introduction

Organelle-targeting fluorescent chemosensing, combined with confocal microscopy, is a promising tool to monitor the key biological molecules at the level of subcellular compartments in live cells and their dynamics for understanding biological processes, which have been well demonstrated for metal ion, intracellular pH, enzyme activities, reactive oxygen species (ROS), and so on.[1,2] Regarding the ROS chemosensors, various organelles have been investigated including mitochondria, nucleus, endoplasmic reticulum (ER), and Golgi apparatus[3]; however, the examples have been mainly focused on mitochondria,[4] probably due to its well-recognized oxidative metabolism and the clear mitochondria targeting strategy, incorporation of positively charged large hydrophobic moiety to the sensors' structures. In fact, ER is another oxidatively active organelle with diverse oxidative metabolisms including oxidative folding of the newly synthesized proteins; yet, the ROS sensors for ER are rarely reported.[5]

ER is the primary organelle responsible for oxidative protein folding and post-translational modifications of proteins, and, of course, for their packing trafficking.[6] The redox balance is slightly biased to oxidation-side relative to those of other organelles and under delicate controlling systems. Indeed, any perturbing factors against the balance may result in accumulation of unfolded proteins in its lumen, causing ER stress, followed by the unfolded protein responses.[7] Undoubtedly, such malfunction of the ER is closely related with various human diseases such as diabetes, inflammation, and neurodegenerative disorders including Alzheimer's disease, Parkinson's disease, and bipolar disorder.[8] Recently, biological studies imply that the ER stress may involve ROS formation in ER,[9] thereby, direct monitoring the ROS levels under ER stress would be highly desirable. Therefore, development of ER-targeting ROS chemosensors would be a challenging topic in the field of fluorescent chemosensors.

Our strategy for ER-targeting fluorogenic ROS chemosensor was shown in Scheme 1, adopting 2′,7′-dichlorodihydrofluorescein diacetate (DCFH DA) and glibenclamide as an ROS sensor and ER-targeting unit, respectively. Dihydrofluorescein unit is highly susceptible for fluorogenic oxidation reactions, thereby, DCFH DA unit has been widely used to measure the cellular ROS levels[10] although its subcellular localization is unclear.[11] And, glibenclamide is a well-known ER guiding unit as demonstrated in many commercially available ER-selective markers (*e.g.*, ER-Tracker™ Green/Red) and its ER targeting ability has been confirmed in one of our recent publications[12] (See Supporting Information Scheme S1 for the molecular structures of DCFH DA and N_3-glibenclamide). Herein, ER-Flu DA was prepared by copper(I)-catalyzed alkyne-azide cycloaddition (CuAAC) reaction between

[†]These authors contributed equally to this work.

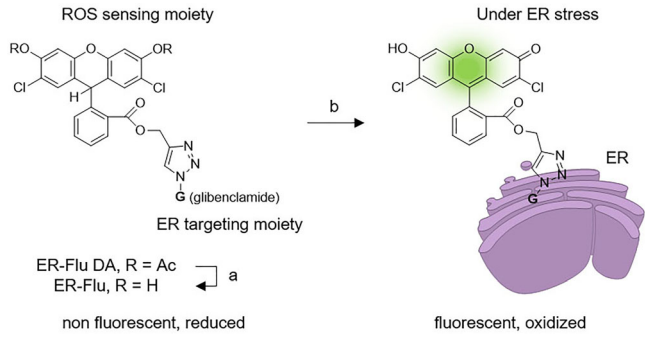

Scheme 1. Schematic representation of ER-targeting fluorogenic ROS chemosensor (ER-Flu) in cells. ER-Flu has two states: Non-fluorescent, reduced form (left) and fluorescent, oxidized form (right). Two stepwise reactions for ER-Flu: (a) deacetylation by esterases. (b) Oxidation by ROS. Ac = acetyl.

3-propargyl ester of DCFH DA and N_3-glibenclamide. The ROS sensing capability of ER-Flu in the live cells and its ER localization were confirmed by confocal experiments in the cellular ER stress models using thapsigargin, brefeldin A, and tunicamycin.

Materials and Experiments

Materials. 2′,7′-Dichlorodihydrofluorescein diacetate (D6883), fluorescein (46955), hematin (porcine, H3281), Dulbecco's modified Eagle's medium (DMEM) (D6429, high glucose), menadione (M5625), brefeldin A (B6542), thapsigargin (T9033), tunicamycin (T7765), and protease inhibitor cocktail (P8340 for use with mammalian cell and tissue extracts) were purchased from Sigma-Aldrich. HeLa (species: human, tissue: cervix, cell type: epithelial, disease: adenocarcinoma, ATCC® CCL-2™). Fetal bovine serum (FBS, Gibco™, 12483-020), ER-Tracker™ Red (E34250), LysoTracker™ Deep Red (L12492), and MitoTracker™ Deep Red FM (M22426) were purchased from Thermo-Fisher Scientific.

Synthesis and Characterization. The synthesis and characterization of dihydrofluorescein diacetate (Flu-acid DA), dihydrofluorescein methyl ester (Flu-ester), and DCFH-propargyl ester DA were summarized in Supporting Information S1. N_3-glibenclamide was prepared by our previous report.[12] ER-Flu DA was prepared following the procedure below.

DCFH-propargyl ester DA (20.0 mg, 0.038 mmol) was dissolved in 3 mL of THF/water (2:1, v/v), and N_3-glibenclamide (20.4 mg, 0.038 mmol) was added to the solution. A 1:1 (v/v) mixture of $CuSO_4$ (60 mM in water) and TBTA (60 mM in THF/ethanol (4:1, v/v)) were prepared. Then, the Cu^{2+}/TBTA cocktail (63 μL) and sodium ascorbate (36 μL, 50 mM) were added to the reaction mixture. After stirring at room temperature at 2 h, the solvent was removed by rotary evaporation. The residual was purified by silica gel column chromatography using hexane/ethyl acetate (1:2, v/v) to yield the desired product (15 mg, 0.014 mmol, yield: 37%). ^{1}H NMR (300 MHz, $CDCl_3$): δ 8.17 (s,1H), 8.07 (d, J = 2.8 Hz, 1H), 7.93 (d, J = 7.9 Hz, 1H), 7.80 (d, J = 2.8 Hz, 1H), 7.74 (d, J = 8.2 Hz, 2H), 7.51 (app br, 2H), 7.38–7.36 (overlapped, 1H), 7.33–7.35 (app d, J = 8.2 Hz, 2H), 7.25–7.23 (app t, 1H), 7.04 (d, J = 7.5 Hz, 1H), 6.91 (s, 2H), 6.86 (s, 2H), 6.38 (app br, 1H), 6.35 34 (app s, 1H), 5.56 (s, 2H), 3.75–3.68 (m, 2H), 3.58–3.55 (m, 1H), 3.19 (s, 3H), 2.98 (t, J = 7.14 Hz, 2H), 2.25 (s, 6H), 1.76–1.08 (m, 10H); ^{13}C NMR (75 MHz, $CDCl_3$): δ 168.2, 167.4, 163.0, 150.6, 149.2, 148.7, 146.1, 145.8, 145.1, 143.2, 138.0, 133.5, 132.1, 131.5, 130.9, 130.6, 130.4, 129.5, 129.2, 128.8, 128.5, 127.4, 127.3, 125.8, 122.8, 121.3, 111.9, 62.3, 58.3, 49.0, 40.6, 37.8, 35.2, 32.8, 25.3, 24.4, 20.5; HR-MS (FAB+): calculated 1058.188 (100.0%) for $C_{50}H_{45}{}^{35}Cl_3N_6O_{12}S$, 1060.185 (95.9%) for $C_{50}H_{45}{}^{35}Cl_2{}^{37}ClN_6O_{12}S$, observed 1059.194 (93.4%), 1061.202 (100%) for $[M + H]^+$.

Deacetylation of Dihydrofluorescein Derivatives

Deacetylation. Each probe stock solution was diluted in methanol (90 μL) to give the final concentration (1 mM). Each probe solution (100 μL, 1 mM) was added to a deoxygenated NaOH solution (400 μL, 10 mM) and the reaction mixture was incubated in Eppendorf ThermoMixer (37°C, 1000 rpm for 30 min). The reaction was checked by TLC (dichloromethane: methanol = 10:1, v/v). To quench the reaction, 1X PBS (2 mL) was added to the reaction.

RP HPLC analysis: Column condition: flow rate = 1 mL/min; solvent A = acetonitrile, solvent B = 0.1% trifluoroacetic acid in water; a linear gradient of solvent B, 0–90% over 30 min; DAD detection at 280 nm.

ROS Experiment of Flu-Acid and Flu-Ester. The preparation of ROS was summarized at Supporting Information S3. Potassium superoxide (KO_2, 14 058), hydrogen peroxide (H_2O_2, 33 323), sodium nitroferricyanide(III) dehydrate (A15656), sodium hypochlorite (NaOCl, L14709) and *tert*-butyl hydroperoxide (A13926) were purchased from Alfa Aesar. Sodium nitrate ($NaNO_3$, 71 752) was purchased from Fluka; Angeli's salt ($Na_2N_2O_3$, 82 23O) from Cayman Chemical; sodium hydroxide pellets (SO620) from Samchun Chemical; isoamyl nitrite (I0089) and diethylenetriamine-pentaacetic acid (D0504) from TCI.

Ester Stability of ER-Flu in Cell Lysate

Cell lysate preparation. HeLa cells were rinsed with 1X PBS two times and harvested (10 000 rpm, 1 min, 4°C). The cells were lysed with cell homogenate buffer (250 mM sucrose, 10 mM HEPES, 1 mM EDTA, protease inhibitor cocktail [1:100; Sigma-Aldrich] [pH 7.4]) using a Dounce homogenizer. The homogenate was centrifuged (10 000 rpm, 15 min, 4°C). The supernatant containing total cell number 15×10^5 in 700 mL was collected for the ester stability analysis.

Sample preparation. The 100 μL of a solution of probe (1 mM in methanol) was added to 400 μL of NaOH (10 mM) and the mixture was incubated at 37°C for 30 min. The reaction was quenched by adding 2 mL of 1X

PBS. The probe solution (250 μL, 40 μM) was added to 1X PBS. Hydrogen peroxide (100 μL, 10 mM) was added to the reaction mixture and then hematin (10 μL, 1 mM) was added. The reaction mixture was incubated in Eppendorf ThermoMixer (37°C, 30 min). The deacetylation and oxidation were confirmed by HPLC.

Cell lysate treatment. The cell lysate (100 μL, 2.1×10^5 cell number) was added to the above sample (200 μL, 10 μM) and then incubated in at 25°C for 30 min. Chilled acetone (800 μL) was added to the mixture and kept in refrigerator (−20°C, 1 h). The sample was centrifuged (11 000 rpm, 15 min, 4 °C). The supernatant was filtered and dried by the stream of N_2 to 200 μL. RP HPLC analysis: flow rate = 1 mL/min; solvent A = acetonitrile, solvent B = 0.1% trifluoroacetic acid in water; a linear gradient of solvent B, 90–65% (0–10 min), 65–15% (10–15 min), 15–0% (15–30 min); DAD detection at 480 nm; FLD detection at excitation 510 nm, emission 528 nm.

Colocalization and ER Stress Experiment. HeLa cells were grown in DMEM supplemented with 10% fetal bovine serum (FBS). For confocal experiments, the cells were plated at 50% confluence on a cover-glass confocal dish and incubated for 24 h. For characterization of the ER-Flu's cellular location, its confocal images were compared to the organelle trackers in the cells treated with menadione (200 μM, 1 h) to increase endogenous ROS level. The cells were co-treated with ER-Flu DA (3 μM) for 30 min and then each organelle tracker (0.3 μM of LysoTracker Deep Red for Lysosome, 0.3 μM of MitoTracker Deep Red for Mitochondria, 1 μM of ER-Tracker Red for ER) for 15 min. The ER-Flu images were obtained by band pass filter (505–550 nm, λ_{ex} = 488 nm) and the organelle tracker images by long pass filter (650 nm ~, λ_{ex} = 633 nm). The Pearson's and Mander's coefficients were calculated using the Auto Quant X3 program. For inducing ER stress, thapsigargin (1 μM), brefeldin A (100 μM), and tunicamycin (20 μg/L) were applied to a separate confocal dish. After 2 h, the cells were treated with ER-Flu DA (3 μM) for 30 min. The confocal images were obtained with a Zeiss LSM510.

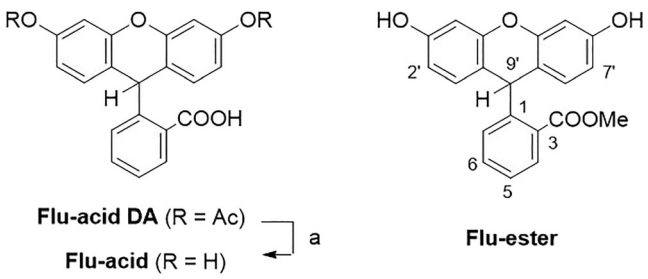

Scheme 2. Molecular structures of the dihydrofluorescein derivatives used in this study. (a) NaOH (10 mM):CH_3OH = 4:1, v/v. The numbering of dihydrofluorescein followed that of fluorescein in the reference 13.

Results and Discussion

In order to investigate the fluorogenic property of dihyrofluorescein ester at the 3-position, we synthesized and characterized Flu-acid DA and Flu-ester (Scheme 2) where the glibenclamide unit is missing and the fluorescein unit has no chloride in the ER-Flu. Many studies on the oxidations and the cellular ROS detection by dihydrofluoresein have been reported.[14] However, derivatization of the carboxyl group at its 3-position was rare and their characterization was investigated.

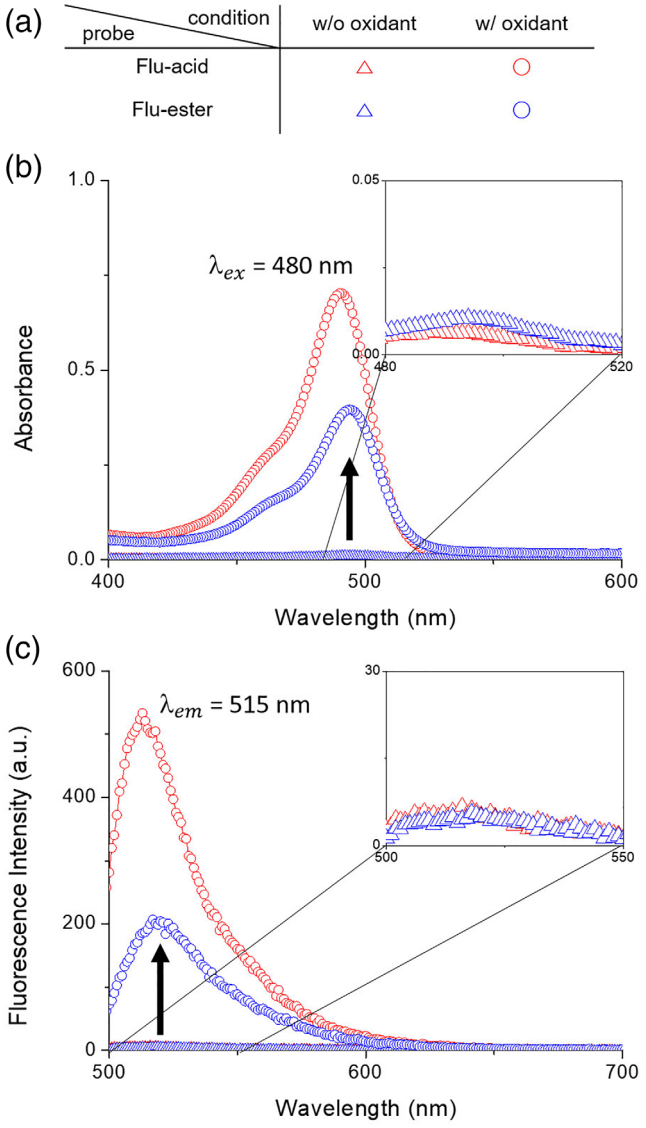

Figure 1. Photophysical response of Flu-acid and Flu-ester under oxidant. (a) Shape and color notation used in this study. (b) Absorption and (c) emission spectra in with and without the H_2O_2/hematin. For absorption spectra, [probe] = 10 μM, [H_2O_2] = 500 μM, [hematin] = 2 μM. For emission spectra, [probe] = [hematin] = 0.5 μM, [H_2O_2] = 25 μM, excitation at 480 nm, ex/em slit width = 1.5/1.5 nm. Reaction time = 1 h. All in 1X PBS.

To avoid auto-oxidation of the Flu-acid, it was freshly deacetylated through basic hydrolysis. The completion of the deacetylation was confirmed by HPLC (Supporting Information Figure S9). Flu-ester was prepared by the direct Zn reduction of fluorescein methyl ester because the ester bond at the 3-position was partially hydrolyzed in the deacetylation condition. The chemical structures were confirmed by ^{1}H NMR and ^{13}C NMR (Supporting Information S1-1).

The UV/vis. absorption and emission changes of Flu-acid/Flu-ester were measured regarding H_2O_2/hematin, which is a well-known oxidation condition to generate hydroxyl radical (•OH) (Figure 1).[15] As shown in the figure, the oxidation generates strong bands at 480 nm in the absorption spectra, and at 515 nm in the emission spectra upon excitation at 480 nm. And, without the oxidant, they showed relatively negligible intensity in absorption or emission spectra. This feature is exactly anticipated from the reactions in Scheme 1.

To investigate the preference of Flu-acid and Flu-ester to various ROS, the fluorogenic activity was measured accordingly (Figure 2). The results showed that the probes are easily oxidized with highly reactive oxygen species such as •OH (hydroxyl radical), ROO• (peroxy radical), $ONOO^-$ (peroxynitrite), and HNO (nitroxyl). However, they were relatively inert to the oxidizing conditions by H_2O_2, O_2•$^-$(superoxide anion radical), and •NO (nitric oxide). These results are in harmony with the anticipation that these fluoresceins have similar reactivities with that of DCFH[16] and that the acid and ester forms have similar preference for the oxidants.[17]

For further characterization of the fluorogenic response of Flu-acid and Flu-ester, various combinations of H_2O_2 and hematin were tested (Supporting Information Figure S10). Flu-ester showed similar reactivity toward H_2O_2 alone, but a little lower toward hematin. Flu-acid was oxidized more quickly than Flu-ester under the H_2O_2/hematin condition. Regarding the oxidation rates (Figure 3), the initial oxidation rate of Flu-ester (S_2) was 4.8 times slower than that of Flu-acid (S_1) in the H_2O_2/hematin condition whereas, in the presence of H_2O_2 only, it was 1.6 times faster than S_1. As seen in Figures 2 and 3; Supporting Information Figure S10, although the reactivity of Flu-ester to various oxidants was quite similar to that of its acid form, it was slightly less reactive.

In order to design a new ER-targeting fluorogenic ROS chemosensor based on modular approach, DCFH was adopted as the ROS sensor instead of dihydrofluorescein. Because of the lower pK_a of the reaction product where the values for 2′,7′-dichlorofluorescein and fluorescein were 5.0 and 6.7,[11] DCFH's emission may be relatively free from

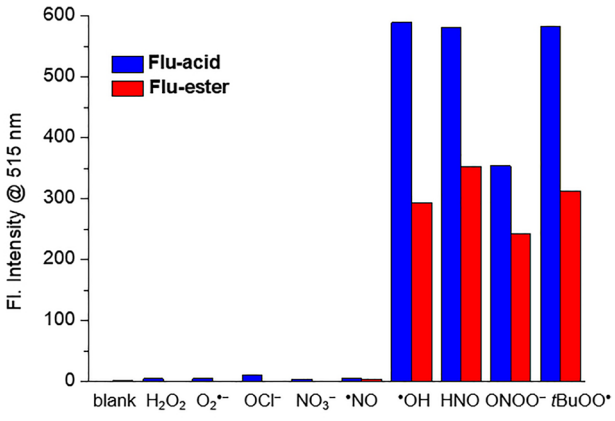

Figure 2. Fluorogenic responses of Flu-acid and Flu-ester in various ROS conditions: H_2O_2 (50 μM), $O_2^{\bullet-}$ (50 μM), OCl^- (10 μM), NO_3^- (50 μM), •NO (50 μM), •OH (50 μM of H_2O_2 + 0.5 μM of hematin), HNO (50 μM), $ONOO^-$(3.5 μM), t-BuOO• (50 μM of TBHP + 0.5 μM of hematin). [Probe] = 0.5 μM, all in 1X PBS. The samples were incubated at 37°C for 30 min and measured for fluorescence intensity with excitation at 480 nm, emission at 515 nm, ex/em slit width = 1.5/1.5 nm.

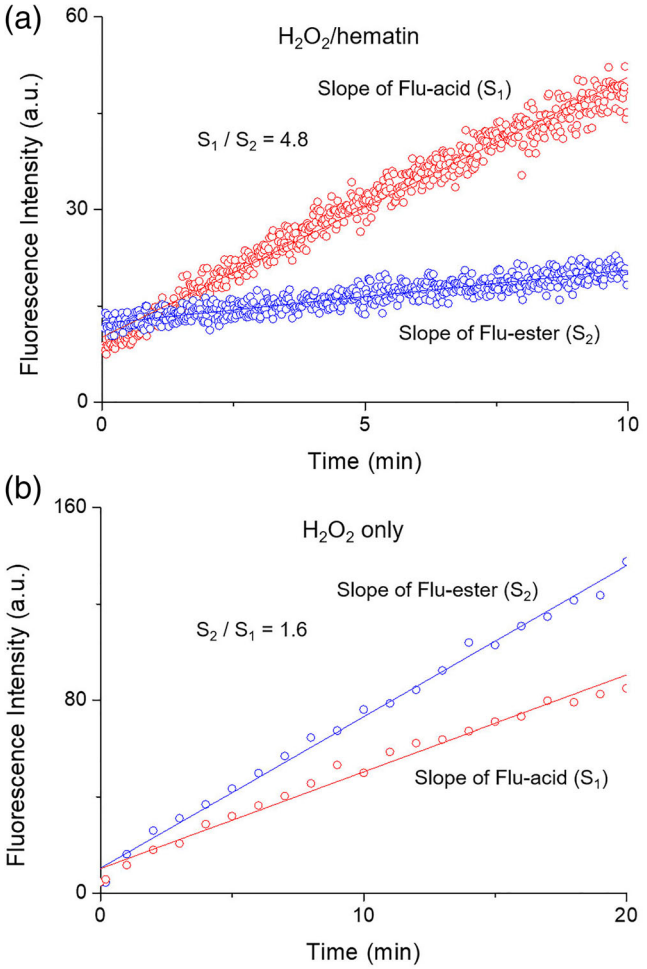

Figure 3. Initial oxidation rate measurements of Flu-acid and Flu-ester. The color definition follows Figure 1(a) (red = Flu-acid, blue = Flu-ester). (a) H_2O_2/hematin condition: [H_2O_2] = 50 μM, [hematin] = 0.5 μM. (b) H_2O_2 only condition, [H_2O_2] = 2.5 mM. All in 1X PBS. Excitation at 480 nm, emission at 515 nm, ex/em slit width = 1.5/1.5 nm.

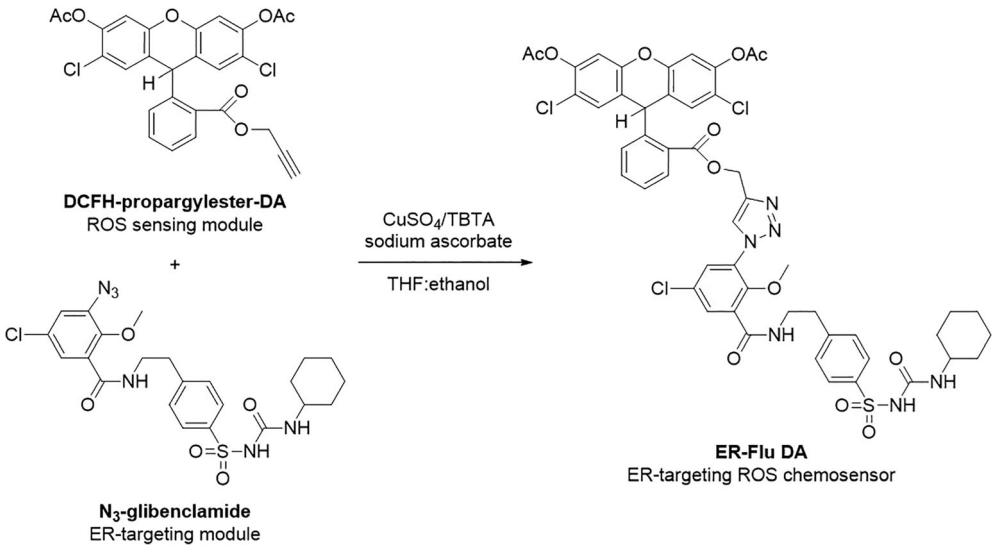

Scheme 3. Synthetic scheme for ER-Flu DA. TBTA,Tris[(1-benzyl-1H-1,2,3-triazol-4-yl)methyl]amine

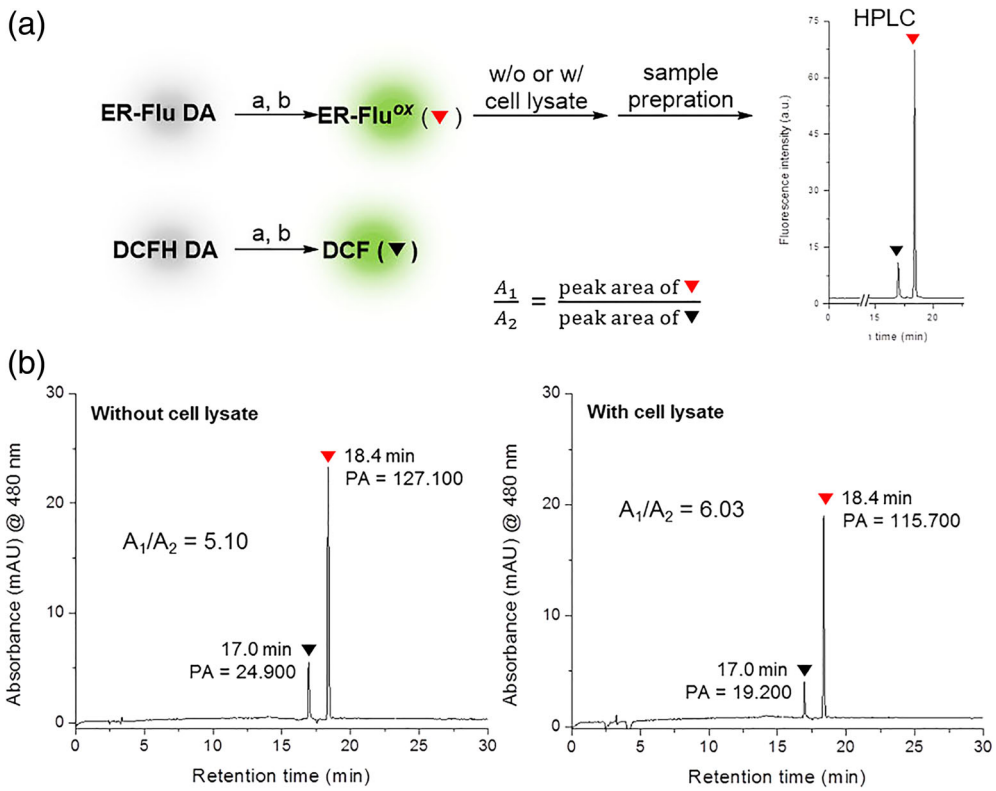

Figure 4. Inner ester bond stability of ER-Flu in cell lysate. (a) Scheme for sample preparation through a) deacetylation (NaOH (10 mM): CH_3OH = 4:1, v/v), b) oxidation (H_2O_2/hematin) and HPLC analysis. (b) HPLC chromatograms of ER-Fluox without or with cell lysate. G = glibenclamide, [probe] = 10 μM.

pH emission around pH 7.0. DCFH-propargyl ester DA was prepared using DCC/DMAP coupling of DCFH DA and propargyl alcohol. Then, ER-Flu DA was synthesized by CuAAC reaction between DCFH-propargyl ester DA (an ROS sensing module) and N_3-glibenclamide (an ER-targeting module) (Scheme 3). The synthesis of DCFH-propargyl ester DA and ER-Flu DA was confirmed by ^{1}H NMR, ^{13}C NMR, and HR-MS (Supporting Information S1-2). The deacetylation of ER-Flu DA was confirmed by HPLC (Supporting Information Figure S11

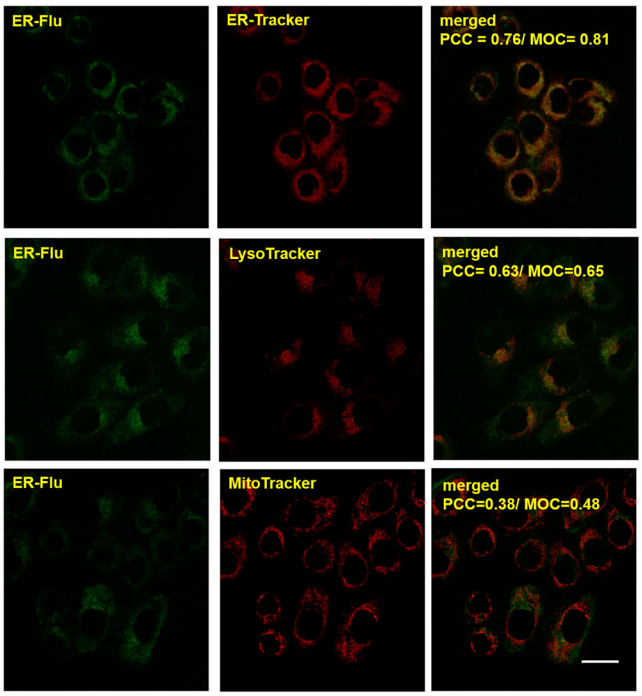

Figure 5. Colocalization experiments using ER-Flu in HeLa cells in the presence of menadione. Fluorescence images of HeLa cells incubated with ER-Flu (left column) and various trackers (middle column). Overlay of left and middle columns (right column). The cells were preincubated in DMEM media containing menadione (200 μM, 1 h) at 37°C. Each sample was treated with ER-Flu DA (3 μM) for 30 min before visualization. Green cell images were obtained using excitation 488 nm and emission BP 505–550 nm. Each sample was treated with the organelle tracker (1 μM) for 15 min before visualization. Red cell images were obtained using excitation 633 nm and emission LP 650 nm. All the images were obtained in the same microscope settings. Scale bar is 20 μm.

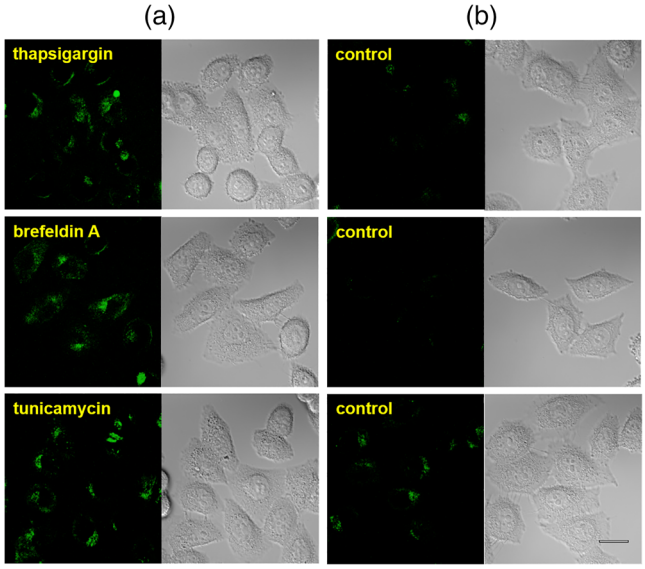

Figure 6. Fluorescence changes of ER-Flu at various ER stress conditions. Column a: with ER stress, column B: without ER inducer. Left image: Fluorescence, right image: Bright field. HeLa cells were preincubated in DMEM media containing ER stress inducer (thapsigargin, 1 μM; brefeldin A, 100 μM; tunicamycin, 20 μg/mL) for 2 h at 37°C. Each sample was incubated with ER-Flu DA for 30 min before visualization. Images of the cells were obtained using excitation 488 nm and emission BP 505–550 nm. All the images were obtained in the same microscope settings. Scale bar is 20 μm.

(a) and (b)). ER-Flu showed similar fluorogenic response under the oxidant condition (H_2O_2/hematin), like Flu-ester (Supporting Information Figure S13).

Prior to ROS measurement in live cells using ER-Flu, its stability in biological systems was pursued, particularly regarding the robustness of ester bond at the 3-position of the fluorescein unit. The enzymatic cleavage of the inner ester bond was monitored by HPLC of the deacetylated, oxidized product (ER-Flu^{ox}) in cell lysate (Figure 4(a)). The stepwise acetylation and oxidation of ER-Flu DA were confirmed by HPLC and the peaks at 17.0, 18.4 min were assigned to DCF and the oxidized form of ER-Flu (ER-Flu^{ox}), respectively (Supporting Information Figures S11–S13). The HeLa cell lysate with esterase activity was prepared following our previous report (Dounce homogenizer, cell homogenate buffer: 250 mM of sucrose, 10 mM of HEPES, 1 mM of EDTA, protease inhibitor cocktail [1:100] [pH 7.4]).[18] ER-Flu^{ox} was treated without or with cell lysate. After acetone precipitation, the supernatant was analyzed by HPLC. The DCF peaks of the samples resulted from the partial hydrolysis of ER-Flu at the deacetylation step. As seen in Figure 4(b), without or with cell lysate condition did not give any significant difference to the peak area ratio between ER-Flu^{ox} (A_1, ▼) and DCF (A_2, ▼) (A_1/A_2 = 5.1 without cell lysate vs. 6.0 with cell lysate). These results supported that the inner ester bond of ER-Flu will also be not cleaved by cellular esterase.

To identify the cellular location of ER-Flu, colocalization experiments were conducted in the presence of organelle trackers (ER, lysosome [Lyso], mitochondrion [Mito]) using confocal microscopy. As seen in Figure 5, the fluorescence images from ER-Flu of HeLa cells treated with menadione better overlapped that of the ER-Tracker compared with that of LysoTracker or MitoTracker (Pearson's correlation coefficients [PCC]: 0.76, 0.69, 0.38 and Mander's overlap coefficients [MOC]: 0.81, 0.68, 0.48, respectively). These dominant ER overlap of ER-Flu in menadione treatment suggested that the fluorogenic oxidation reaction of ER-Flu with ROS occurred mainly in the ER.

Considering the essential roles of ROS in oxidative stress, the fluorogenic ROS reaction of ER-Flu, confined to the ER, was investigated in the context of ER stress. ER-Flu DA was applied to the cells treated with one of three ER stress inducers: thapsigargin,[19] brefeldin A,[20] or tunicamycin.[21] Whereas all of these inhibitors induce the unfolded protein response, a typical feature of ER stress, their mechanisms of action differ; disturbing Ca^{2+} ion

homeostasis, blocking protein trafficking from ER to Golgi apparatus, and unfolded protein accumulation, respectively. As seen in Figure 6, the fluorescence intensity of ER-Flu is increased in the presence of each of the ER stress inducers, indicating that the ROS level in the ER was significantly increased under the ER stress conditions. These results imply that the oxygen-related metabolisms may be highly coordinated with the physiological processes such as *de novo* protein synthesis, folding and so on. However, any further investigation may beyond the scope of this work.

Conclusion

We introduced an ER-targeting fluorogenic ROS chemosensor (ER-Flu) as an example of derivatization of the carboxyl group at 3-position in the dichlorodihydro-fluorescein. The acetylated ER-Flu was synthesized by a CuAAC reaction between DCFH-propargyl ester DA (a ROS sensing unit) and N_3-glibenclamide (an ER guiding unit). We found that esterification of the 3-position does not significantly change the reactivity toward the oxidants, just slight attenuation. The inner ester bond at the 3-position was stable in the cell lysate. Finally, by confocal colocalization, the probe locates in the ER of the live cells and readily reacts with ROS species. Taking advantages of its ROS sensing capability in ER, we demonstrated that large amounts of ROSs can be generated by disturbance of ER function, shown in the ER stress models by thapsigargin, brefeldin A, and tunicamycin.

Acknowledgments. This work was supported by NRF Korea Research Fellowship Program (2019H1D3A1A02071159, HTL), NRF (2017R1A2A2A05069805, CK), and NRF (2017R1D1A1B03034972, TWK) grant funded by the Ministry of Science and ICT through the National Research Foundation of Korea.

Supporting Information. Additional supporting information may be found online in the Supporting Information section at the end of the article.

References

1. Y. Kurishita, T. Kohira, A. Ojida, I. Hamachi, *J. Am. Chem. Soc.* **2012**, *134*, 18779.
2. H. Zhu, J. Fan, J. Du, X. Peng, *Acc. Chem. Res.* **2016**, *49*, 2115.
3. W. Xu, Z. Zeng, J. H. Jiang, Y. T. Chang, L. Yuan, *Angew. Chem. Int. Ed. Engl.* **2016**, *55*, 13658.
4. B. C. Dickinson, D. Srikun, C. J. Chang, *Curr. Opin. Chem. Biol.* **2010**, *14*, 50.
5. a) Y. Tang, A. Xu, Y. Ma, G. Xu, S. Gao, W. Lin, *Sci. Rep.* **2017**, *7*, 12944. b) Q. Meng, H. Jia, P. Succar, L. Zhao, R. Zhang, C. Duan, Z. Zhang, *Biosens. Bioelectron.* **2015**, *74*, 461.
6. G. M. Cooper, The Endoplasmic Reticulum. In *The Cell: A Molecular Approach*, 2nd ed., Sinauer Associates, Sunderland, MA, **2000**.
7. C. Hetz, *Nat. Rev. Mol. Cell Biol.* **2012**, *13*, 89.
8. H. Yoshida, *FEBS J.* **2007**, *274*, 630.
9. S. S. Cao, R. J. Kaufman, *Antioxid. Redox Signal.* **2014**, *21*, 396.
10. X. Chen, Z. Zhong, Z. Xu, L. Chen, Y. Wang, *Free Radic. Res.* **2010**, *44*, 587.
11. D. B. Zorov, C. R. Filburn, L. O. Klotz, J. L. Zweier, S. J. Sollott, *J. Exp. Med.* **2000**, *192*, 1001.
12. Y. Wi, H. T. Le, P. Verwilst, K. Sunwoo, S. J. Kim, J. E. Song, H. Y. Yoon, G. Han, J. S. Kim, C. Kang, T. W. Kim, *Chem. Commun.* **2018**, *54*, 8897.
13. A. G. Stephen, K. M. Worthy, E. Towler, J. A. Mikovits, S. Sei, P. Roberts, Q. E. Yang, R. K. Akee, P. Klausmeyer, T. G. McCloud, L. Henderson, A. Rein, D. G. Covell, M. Currens, R. H. Shoemaker, R. J. Fisher, *Biochem. Biophys. Res. Commun.* **2002**, *296*, 1228.
14. A. Aranda, L. Sequedo, L. Tolosa, G. Quintas, E. Burello, J. V. Castell, L. Gombau, *Toxicol. in Vitro* **2013**, *27*, 954.
15. R. Cathcart, E. Schwiers, B. N. Ames, *Anal. Biochem.* **1983**, *134*, 111.
16. K. Setsukinai, Y. Urano, K. Kakinuma, H. J. Majima, T. Nagano, *J. Biol. Chem.* **2003**, *278*, 3170.
17. P. Wardman, *Free Radic. Biol. Med.* **2007**, *43*, 995.
18. S. J. Park, H. W. Lee, H. R. Kim, C. Kang, H. M. Kim, *Chem. Sci.* **2016**, *7*, 3703.
19. O. Thastrup, P. J. Cullen, B. K. Drobak, M. R. Hanley, A. P. Dawson, *Proc. Natl. Acad. Sci. U. S. A.* **1990**, *87*, 2466.
20. Y. Misumi, Y. Misumi, K. Miki, A. Takatsuki, G. Tamura, Y. Ikehara, *J. Biol. Chem.* **1986**, *261*, 11398.
21. A. D. Elbein, *Rev. Biochem.* **1984**, *16*, 21.

